Digital Communications and Networks (2015) 1, 161–170

HOSTED BY

ELSEVIER

Available online at www.sciencedirect.com

ScienceDirect

journal homepage: www.elsevier.com/locate/dcan

DCN Digital Communications and Networks

Joint optimization of spectrum and energy efficiency in cognitive radio networks

Shaowei Wang[a,*], Chonggang Wang[b,1]

[a]School of Electronic Science and Engineering, Nanjing University, Nanjing 210023, China
[b]InterDigital Communications, 781 Third Avenue, King of Prussia, PA 19406, USA

Received 7 July 2015; received in revised form 7 September 2015; accepted 14 September 2015
Available online 30 September 2015

KEYWORDS
Cognitive radio;
Energy efficiency;
Multi-objective optimization;
Spectrum efficiency

Abstract
In this paper, we discuss the joint improvement of the energy efficiency (EE) and the spectrum efficiency (SE) in OFDM-based cognitive radio (CR) networks. A multi-objective resource allocation task is formulated to optimize the EE and the SE of the CR system simultaneously with the consideration of the mutual interference and the spectrum sensing errors. We first exploit the EE–SE relations and demonstrate that the EE is a quasiconcave function of the SE, based on which the Pareto optimal set of the multi-objective optimization problem is characterized. To find a unique globally optimal solution, we propose a unified EE-SE tradeoff metric to transform the multi-objective optimization problem into a single-objective one which has a D.C. (difference of two convex functions/sets) structure and yields a standard convex optimization problem. We derive a fast method to speed up the time-consuming computation by exploiting the structure of the convex problem. Simulation results validate the effectiveness and efficiency of the proposed algorithms, which can produce the unique globally optimal solution of the original multi-objective optimization problem.
© 2015 Chongqing University of Posts and Telecommunications. Production and Hosting by Elsevier B.V. This is an open access article under the CC BY-NC-ND license (http://creativecommons.org/licenses/by-nc-nd/4.0/).

1. Introduction

Spectrum scarcity crisis exists for many wireless applications, especially in the band below 6 GHz. On the other hand, investigations show that large portions of spectrum are highly underutilized due to inefficient conventional regulatory policies [1]. Cognitive Radio (CR) is deemed as a highly promising technology to improve the spectrum usage efficiency and has gained more and more attentions in recent years [2-4]. CR technology has been proposed as a solution to the underutilization problem by allowing Secondary Users (SUs) to sense radio spectrum environment and opportunistically access licensed frequency, as long as the interference to the Primary Users (PUs) can be kept under their tolerances, such as interference temperature. In order to meet the requirements of opportunistic access, the physical layer of a CR system should be very flexible, which

*Corresponding author.
E-mail address: wangsw@nju.edu.cn (S. Wang).
[1]Tel.: +86 13337816198.

http://dx.doi.org/10.1016/j.dcan.2015.09.004
2352-8648/© 2015 Chongqing University of Posts and Telecommunications. Production and Hosting by Elsevier B.V. This is an open access article under the CC BY-NC-ND license (http://creativecommons.org/licenses/by-nc-nd/4.0/).

necessitates multicarrier methods to operate in CR networks. Orthogonal Frequency Division Multiplexing (OFDM) has been widely recognized as a fascinating air interface for CR systems due to its flexibility in adapting spectral environments and allocating radio spectrum among SUs, which is the prerequisite for the CR system to acquire high performance [5].

Resource Allocation (RA) is one of the most important problems in OFDM-based wireless networks and has been studied extensively for more than a decade. A survey can be found in [6]. Spectral efficiency (SE), defined as the system throughput per unit of bandwidth, is a widely accepted criterion for wireless network optimization. For OFDM-based CR networks, there are many research results on how to improve the system performance from the SE perspective in the literature.

In [7], a balanced strategy for OFDMA radio resource allocation based on game theory concepts is presented. The proposed approach, explicitly addressing users perceived quality, ensures high balance between efficiency and fairness. In [8], an efficient algorithm is proposed to allocate bits among all OFDM subchannels in CR systems. The proposed algorithm can obtain the optimal solution with low computational complexity in most cases. In [9], both real-time and non-real-time services are considered, and fast RA algorithms are developed. However, fairness among users is ignored in [9], as well as spectrum sensing issue. In [10], a general RA framework in CR networks is developed, as well as efficient algorithms, which hint that RA in OFDM-based CR networks can be tackled effectively and efficiently by exploiting the structure of the considered problem.

On the other hand, the energy consumption of information and communications technology (ICT) has recently become an economic issue for operators as well as a big challenge for sustainable development [11]. With vast and rapid deployment of fourth generation (4G) networks, as well as the 5G vision of a totally connected world, the energy consumption is also growing at a staggering rate nowadays, which results in a large amount of greenhouse gas and high operation expenditure for wireless service providers. Green communication, which emphasizes on incorporating energy awareness in communication systems, is becoming more and more important [12]. Thus, energy-efficient RA has attracted much attention in both industry and academia, especially for the OFDM-based system which is the most promising modulation technique for the future wireless networks. Different from the throughput-oriented RA targets, energy efficient RA aims at maximizing the energy efficiency of wireless networks. An adequate energy-efficient metric should be given primary importance in overall energy-efficient network design, since it is related to the optimized decisions directly. The most popular one is called '*bits-per-Joule*', which is defined as the system throughput for unit-energy consumption. Recently, more and more researches have been carried out in the literature on energy-efficient wireless networks, and diverse technologies have been proposed in all aspects, trying to close the gap between practice and expectations.

In [13], an energy saving algorithm for spectrum sensing stage in cognitive radio networks is proposed and the detection accuracy over the desirable bound is maintained. In [14], green cellular operation is discussed. Using real data traces, [14] derived a first-order approximation of the percentage of power saving one can expect by turning off base stations during low traffic periods while maintaining coverage. In [15], the problem of non-cooperative resource allocation in multi-cell uplink OFDMA systems with multiple base station antennas is considered. In [16], a greedy energy-efficient BS deployment framework is developed for HetNets. The proposed algorithm deploys micro-BSs iteratively and maximizes the energy efficiency of the network. Ref. [17] analyzed three geographical adaptive fidelity models to optimize energy consumption in vehicular ad hoc networks. The relationship between the number of network grids and energy consumption is derived.

Both EE and SE are important for RA design. While it is noteworthy that there is only limited work on the joint optimization of EE and SE for wireless communication networks. The problem is that EE and SE do not always coincide and may even conflict sometimes [18]. The traditional approach to increase SE by trading off the transmit power for limited bandwidth results in reduced EE. Moreover, when the circuitry power factors are incorporated, the tradeoff relationship achieved between SE and EE is not quite straightforward. In fact, to develop a systematic way to find the remaining gaps for further optimization, a unified framework is needed. This is the fundamental framework of the EE and SE trade-off, which has long been pointed out by Shannon's ground-breaking theory but has yet to be fully utilized. The EE–SE trade-off analysis offers a balanced view to the nature of a communication system and provides guidelines for wireless system design and optimization. In [19], four selected green transmission technologies solutions are introduced, focusing on how to utilize the degrees of freedom in different resource domains, as well as how to balance the tradeoff between energy and spectrum efficiency. In [20], the EE–SE trade off optimization problem in downlink orthogonal frequency division multiple access (OFDMA) networks is formulated to maximize EE with a minimal SE requirement. In [21], a multi-criteria optimization problem is proposed to investigate the relationship between EE and SE in distributed antenna systems. The multi-criteria optimization problem is solved by using the weighted sum method. In [22], the EE and SE is simultaneously optimized and a unified metric for EE-SE tradeoff design in point-to-point wireless networks is proposed. However, EE–SE relation for OFDM-based CR networks is more complicated. In addition to the constraint that the interference to the PUs should be restricted, spectrum sensing errors should also be taken into consideration. In fact, perfect spectrum sensing is too difficult to acquire in practical wireless scenarios, and thus, RA with imperfect spectrum sensing is worth noting. How to allocate system resource to tradeoff EE and SE efficiently in OFDM-based CR networks is a nontrivial question.

In this paper, we formulate a multi-objective optimization problem to optimize EE and SE simultaneously. The mutual interference and the spectrum sensing errors are taken into consideration in our system model. We first prove that EE is quasiconcave in SE in the proposed system model. The Pareto optimal set of the multi-objective optimization problem is then characterized. To find a unique globally optimal solution, we proposed a unified EE–SE trade off metric to transform the multi-objective optimization problem into a single-objective one. The single-objective optimization problem has a D.C. (difference of two convex functions/sets) structure and can be solved by the proposed Frank-and-Wolfe (FW) procedure. In the FW procedure, a convex optimization problem needs to be solved. We derive a fast barrier method to speed up the time-consuming computation by exploiting the structure of the problem.

The rest of this paper is organized as follows. In Section 2, we illustrate the system model and formulate our optimization task. In Section 2.1, we propose a heuristic subchannel allocation method. In Section 3, we analyze the fundamentals for EE-SE relation and then propose the EE-SE trade off power allocation scheme. Simulation results are given in Section 4, as well as discussions. Finally, we conclude the paper in Section 4.1.

2. System model and problem formulation

Consider the downlink of an OFDM-based CR system with K SUs, denoted by $\mathcal{K}=\{1,2,\ldots,K\}$, coexisting with L active PUs served by a licensed system. The SUs opportunistically use the spectrum licensed by PUs via an access point (AP). Each PU registers part of the licensed spectrum, named as a sub-band. The available bandwidth W is divided into N_t OFDM subchannels in the CR system.

In this paper we assume that perfect channel-state information is available at the transceivers of the SUs and the PUs. Let $\mathcal{M}^l$ denote the set of subchannels corresponding to the sub-band licensed to the lth PU. With periodic spectrum sensing, the CR network identifies non-active frequency bands and selects a subset $\mathcal{N}=\{1,\ldots,N\}$ among the subchannels to transmit information. In other words, only the subchannels in vacant sub-bands can be used by the CR network.

The bandwidth of each subchannel is B and the nominal spectrum of the nth subchannel spans from $f_s+(n-1)B$ to f_s+nB, where f_s is the starting frequency. When the CR system transmits information over the nth subchannel with unit transmission power, the interference introduced to the jth subchannel in the sub-band of the lth PU is [23]

$$I^n_{j,l}=\int_{(j-1)B-(n-1/2)B}^{jB-(n-1/2)B} g_{n,l}\phi(f)\,df, \tag{1}$$

where $g_{n,l}$ is the power gain from the AP to the receiver of the lth PU on the nth subchannel. $\phi(f)=T(\frac{\sin \pi fT}{\pi fT})^2$ is the power spectrum density (PSD) of OFDM signal, T is the OFDM symbol duration.

In practical systems, there are typically two kinds of sensing errors [24]. The first is *misdetection*, which occurs when the CR system fails to detect the PUs' signals. The band of a subchannel is identified to be vacant but it is truly used by the PU. The other kind of sensing errors is *false alarm*, which means the CR network identifies the band of a subchannel is unavailable but it is vacant actually. Generally, the AP in the CR system collects the sensed information of all SUs and makes a decision on which subchannel can be used by SUs. Then the set of sensed available subchannels $\mathcal{M}^l_v$ in the sub-band of the lth PU is determined, as well as the set of sensed unavailable subchannels $\mathcal{M}^l_o$. The probabilities of misdetection and false alarm on the nth subchannel are q^m_n and q^f_n, respectively. The values of q^m_n and q^f_n can be obtained by either local spectrum sensing via the transceivers of SUs, or preferably, cooperative spectrum sensing [24] and distributed spectrum clustering [25]. For a given area, the misdetection and false-alarm probabilities can also be estimated by mining the spectrum usage data to analyze the statistics of the primary traffic pattern [26]. A survey of spectrum sensing and sharing for CR systems can be found in [27].

Obviously, misdetection results in co-channel interference to the PUs, while false alarm lowers the utilization efficiency of spectrum. There are four possible scenarios for spectrum sensing, as shown in Table 1, where $\mathcal{H}_n$ and $\mathcal{O}_n$ are the hypotheses of the absence and the presence of a certain PU's signal on the nth subchannel, $\tilde{\mathcal{H}}_n$ and $\tilde{\mathcal{O}}_n$ are the events that the nth subchannel is available or unavailable based on the sensed information, respectively. Denote $P_{1,n}$ as the probability that the nth subchannel is truly used by a PU while the CR network makes a correct judgement, we have

$$\begin{aligned}P_{1,n}&=P\{\{\mathcal{O}_n|\tilde{\mathcal{O}}_n\}\}\\&=\frac{P\{\tilde{\mathcal{O}}_n|\mathcal{O}_n\}P\{\mathcal{O}_n\}}{P\{\tilde{\mathcal{O}}_n|\mathcal{O}_n\}P\{\mathcal{O}_n\}+P\{\tilde{\mathcal{O}}_n|\mathcal{H}_n\}P\{\mathcal{H}_n\}}\\&=\frac{(1-q^m_n)q^L_n}{(1-q^m_n)q^L_n+q^f_n(1-q^L_n)},\end{aligned} \tag{2}$$

where q^L_n is the priori probability that the sub-band of the nth subchannel is used by PUs. Similarly, let $P_{2,j}$ denote the probability that the jth subchannel is truly occupied when the CR system deems it as vacant.

Then the interference introduced to the lth PU by the access of an SU on the nth subchannel with unit transmission power is

$$I^{SP}_{n,l}=\sum_{j\in\mathcal{M}^l_o}P_{1,j}I^n_{j,l}+\sum_{j\in\mathcal{M}^l_v}P_{2,j}I^n_{j,l}. \tag{3}$$

Define the signal-to-noise ratio (SNR) of the kth SU on the nth subchannel as

$$H_{k,n}=\frac{g^{SS}_{k,n}}{\Gamma(N_0B+\sum_{l=1}^{L}I^{PS}_{k,n,l})}, \tag{4}$$

where $g^{SS}_{k,n}$ is the channel gain between the AP and the receiver of the kth SU over the nth subchannel, N_0 is the PSD of additive white Gaussian noise, Γ is the SNR gap and can be represented as $\Gamma=-\frac{\ln(5BER)}{1.5}$ for an uncoded MQAM with a specified BER [28]. The transmission rate of the nth

Table 1 Probability information from imperfect spectrum sensing.

	Actual state	Sensing result	Probability information
1	Active ($\mathcal{O}_n$)	Occupied ($\tilde{\mathcal{O}}_n$)	$P\{\tilde{\mathcal{O}}_n|\mathcal{O}_n\}=1-q^m_n$
2	Active ($\mathcal{O}_n$)	Vacant ($\tilde{\mathcal{H}}_n$)	$P\{\tilde{\mathcal{H}}_n|\mathcal{O}_n\}=q^m_n$
3	Idle ($\mathcal{H}_n$)	Vacant ($\tilde{\mathcal{H}}_n$)	$P\{\tilde{\mathcal{H}}_n|\mathcal{H}_n\}=1-q^f_n$
4	Idle ($\mathcal{H}_n$)	Occupied ($\tilde{\mathcal{O}}_n$)	$P\{\tilde{\mathcal{O}}_n|\mathcal{H}_n\}=q^f_n$

subchannel used by the kth SU is

$$r_{k,n} = \rho_{k,n} B \log(1 + p_{k,n} H_{k,n}), \tag{5}$$

where $p_{k,n}$ is the kth SU's transmission power on the nth subchannel, $\rho_{k,n}$ can only be either 1 or 0, indicating whether the nth subchannel is used by the kth SU or not.

In this paper, spectrum-efficiency η_{SE} is defined as the system throughput per unit of bandwidth

$$\eta_{SE} = \sum_{n=1}^{N} \sum_{k=1}^{K} \rho_{k,n} \log(1 + p_{k,n} H_{k,n}). \tag{6}$$

Energy-efficiency η_{EE} is defined as the ratio of the SE over the total power consumption

$$\eta_{EE} = \frac{\eta_{SE}}{\sum_{n=1}^{N} \sum_{k=1}^{K} \rho_{k,n} p_{k,n} + P_c}, \tag{7}$$

where P_c is the circuit power consumption which can be a constant [29]. Both the transmission power and the circuit energy consumption are taken into consideration for energy-efficient communication, where the former is used for reliable data transmission and the latter represents average energy consumption of device electronics.

2.1. Problem formulation

Our goal is to simultaneously maximize EE and SE of the CR system which operates in a power-limited situation while keeping the interference to the PUs not exceeding their specified thresholds. Thus, our optimization problem can be formulated as follows:

$$\begin{aligned} &\max_{p_{k,n}, \rho_{k,n}} \{\eta_{SE}, \eta_{EE}\} \\ &\text{s.t.} \quad C1: p_{k,n} \geq 0, \forall k, n \\ &\quad C2: \sum_{n=1}^{N} \sum_{k=1}^{K} \rho_{k,n} p_{k,n} \leq P_t \\ &\quad C3: \sum_{n=1}^{N} \sum_{k=1}^{K} \rho_{k,n} p_{k,n} I_{n,l}^{SP} \leq I_l^{th}, \forall l \\ &\quad C4: \rho_{k,n} \in \{0, 1\}, \forall k, n \\ &\quad C5: \sum_{k=1}^{K} \rho_{k,n} = 1, \forall n. \end{aligned} \tag{8}$$

where P_t is the power limit of the CR system and I_l^{th} is the interference power threshold of the lth PU. C1 is intuitive. C2 and C3 are the power limitation and the interference constraints, respectively. C4 and C5 indicate that all subchannels are not shared among SUs. That is, a subchannel can be only used by one SU.

3. Heuristic subchannel allocation

Eq. (8) defines a mixed integer programming problem that involves both binary variables $\rho_{k,n}$'s and real variables $p_{k,n}$'s for optimization. To make the problem tractable, we propose a two-step procedure to address (8): subchannels allocation and power distribution. The power distribution scheme will be discussed in Section 4.1. In this section, we propose an heuristic subchannels allocation algorithm to figure out the binary variables $\rho_{k,n}$, specifying a subchannels allocation assignment.

In a cognitive OFDM system, there are L interference constraints which should be considered. If the nth subchannel is interference limited [8], the total power allocated to it is not more than $\min_l \{I_l^{th}/I_{n,l}^{SP}\}$. Jointly consider the transmission power and interference threshold constraints, the maximum possible power allocated to the nth subchannel is

$$p_{k,n}^{max} = \min(P_t, \min_l \{I_l^{th}/I_{n,l}^{SP}\}). \tag{9}$$

Denote $r_{k,n}^{\max}$ as the highest achievable rate of the nth subchannel used by the kth SU, we have

$$r_{k,n}^{\max} = B \log(1 + p_{k,n}^{\max} H_{k,n}). \tag{10}$$

The normalized maximum rate is a practicable criterion to measure the QoS of a subchannel, giving insightful hints for subchannel allocation.

To simplify analysis and computation, the power of a subchannel is temperately set as

$$p_{k,n} = \min(P_t/N, \min_l \{I_l^{th}/I_{n,l}^{SP}\}). \tag{11}$$

Let Ω_k denote the subchannel set employed by the kth SU, and $\mathcal{N}$ is the set of subchannels. The outline of our subchannel allocation scheme is described in Table 2. We allocate the N subchannels one by one. While allocating the $n+1$th subchannel, define the normalized change index to allocate the $(n+1)$th subchannel to the kth SU as follows:

$$\eta_\delta^k = \left(\frac{\eta_{SE}^k - \eta_{SE}^n}{\eta_{SE}^n}\right)\left(\frac{\eta_{EE}^k - \eta_{EE}^n}{\eta_{SE}^n}\right), \tag{12}$$

where η_{SE}^n and η_{EE}^n are the SE and the EE corresponding to the allocation scheme of the n subchannels that have already been allocated. η_{SE}^k and η_{EE}^k are the SE and the EE when additionally allocating the $(n+1)$th subchannel to the kth SU. The $(n+1)$th subchannel will be allocated to the SU with maximal η_δ^k.

It is easy to show that the complexity of the proposed heuristic subchannel assignment is approximately $O(KN)$.

Table 2 Subchannel allocation scheme.

Subchannel Allocation Scheme

1.**Initialization:**
2. $\mathcal{N} = \{1, 2, \ldots, N\}$, $\Omega_k = \varnothing, \forall k$, $k^* = 0$, $\eta_{SE}^0 = 0$, $\eta_{EE}^0 = 0$
3. ***For*** *n from* 1 *to N*
4. Set *tmp*=0
5. *For k from* 1 *to K*
6. Calculate η_{SE}^k and η_{EE}^k when subchannel n is added to Ω_k,
7. Calculate η_δ^k.
8. *If* $\eta_\delta^k > tmp$
9. Set $k^* = k$
10. ***Endif***
11. Update $tmp = \eta_\delta^k$
12. ***Endfor***
13. Update $\Omega_{k^*} = \Omega_{k^*} \cup n$
14. Calculate η_{SE}^n and η_{EE}^n.
15. ***Endfor***

4. EE-SE tradeoff power allocation

Since the subchannel assignment is fixed, power allocation can be performed across the assigned subchannels to simultaneously maximize EE and SE. The power allocation problem is as follows:

$$\begin{aligned}&\max_{p_n}\ \{\eta_{SE},\eta_{EE}\}\\ &\text{s.t.}\quad C1: p_n \geq 0, \forall n\\ &\quad C2: \sum_{n=1}^{N} p_n \leq P_t,\\ &\quad C3: \sum_{n=1}^{N} p_n I_{n,l}^{SP} \leq I_l^{th}, \quad l=1,\ldots,L,\end{aligned} \tag{13}$$

where p_n is the transmission power on the nth subchannel.

4.1. Fundamentals for EE-SE relation

We first study the EE-SE relation and demonstrate the quasiconcavity of EE in SE. As the CR system is power-limited and interference-limited, there is a maximum value of η_{SE} [30]. Assume the maximal value of η_{SE} is η_{SE}^{max} and the SE region is $[0,\eta_{SE}^{max}]$.

Theorem 1. *For any given SE, achieved with power allocation matrix P that satisfy all constraints in (13), the maximum EE, $\eta_{EE}^{m}(\eta_{SE})=\max_P \eta_{EE}(\eta_{SE})$, is strictly quasiconcave in η_{SE}. Moreover, in the SE region $[0,\eta_{SE}^{max}]$, the EE $\eta_{EE}^{m}(\eta_{SE})$*

(i) *strictly increases with η_{SE} and is maximized at $\eta_{SE}=\eta_{SE}^{max}$ if $\frac{d\eta_{EE}^{m}(\eta_{SE})}{d\eta_{SE}}|_{\eta_{SE}=\eta_{SE}^{max}} \geq 0$,*
(ii) *first strictly increases and then strictly decreases with η_{SE} and is maximized at $\eta_{SE}=\eta_{SE}^{*}$ if $\frac{d\eta_{EE}^{m}(\eta_{SE})}{d\eta_{SE}}|_{\eta_{SE}=\eta_{SE}^{max}} < 0$, where $\eta_{SE}^{*}=\text{argmax}\ \eta_{EE}^{m}(\eta_{SE})$.*

The proof of Theorem 1 is in Appendix A. From Theorem 1, the EE is quasiconcave in SE in this CR system model and there are two possible EE-SE curves. The EE-SE curves can be obtained by solving the following optimization problem:

$$\begin{aligned}&\max_{p_n}\ \eta_{EE}\\ &\text{s.t.}\quad C1: \eta_{SE}=C,\\ &\quad C2: \sum_{n=1}^{N} p_n I_{n,l}^{SP} \leq I_l^{th}, \quad l=1,\ldots,L\\ &\quad C3: p_n \geq 0, \forall n.\end{aligned} \tag{14}$$

If we enumerate all possible C and calculate the corresponding optimal solutions of (14), we obtain EE-SE curves.

Then we introduce the concept of Pareto optimal solution, which is a basic concept in multi-object optimization problem. Feasible solution P_1 is called to dominate feasible solution P_2, if $\eta_{SE}(P_1)\geq\eta_{SE}(P_2)$ and $\eta_{EE}(P_1)\geq\eta_{EE}(P_2)$. A feasible solution P_0 is called Pareto optimal if there is no other feasible solution dominating it. There may be multiple Pareto optimal solutions for the multi-object optimization problem. The Pareto optimal set is the set of all Pareto optimal points.

Theorem 2. *The Pareto optimal set of problem (13) is*

$$P^{POS}=\begin{cases}\{P|\eta_{SE}^{*}\leq\eta_{SE}\leq\eta_{SE}^{max}\} & \text{if } \eta_{SE}^{*}<\eta_{SE}^{max}\\ P|\eta_{SE}=\eta_{SE}^{max} & \text{if } \eta_{SE}^{*}\geq\eta_{SE}^{max}\end{cases}. \tag{15}$$

Theorem 2 is proved in Appendix B. According to (15), in the case of $\eta_{SE}^{*}\geq\eta_{SE}^{max}$, P^{POS} contains a single point, which means that the globally optimal solution for (13) is unique. So we only need to analyze the case of $\eta_{SE}^{*}<\eta_{SE}^{max}$.

4.2. EE and SE tradeoff meric

To facilitate system design, we should try to find a unique global solution from the Pareto optimal set P^{POS}. Scalarization method is efficient to distinguish a unique point in the Pareto optimal set. We can transform the multi-object optimization problem (13) into a single-object optimization problem by scalarization methods.

Define a EE and SE tradeoff metric [22] as

$$U(P)=[\eta_{SE}(P)]^{\omega}\times[\eta_{EE}(P)]^{1-\omega}, \tag{16}$$

where $\omega\in[0,1]$. $(\omega,1-\omega)$ is a given preference configuration for SE and EE. $U(P)$ is referred as the utility function.

Then (13) can be transformed into the following single-object optimization problem

$$\begin{aligned}&\max_{p_n}\ U(P)\\ &\text{s.t.}\quad C1: p_n \geq 0, \forall n\\ &\quad C2: \sum_{n=1}^{N} p_n \leq P_t,\\ &\quad C3: \sum_{n=1}^{N} p_n I_{n,l}^{SP} \leq I_l^{th}, \quad l=1,\ldots,L.\end{aligned} \tag{17}$$

4.3. D.C. programming

Do the following utility transformation:

$$\begin{aligned}V(P)&=\log U(P)\\ &=\omega\log\eta_{SE}(P)+(1-\omega)\log\eta_{EE}(P)\\ &=\log\eta_{SE}(P)-(1-\omega)\log(P_{sum}+P_c),\end{aligned} \tag{18}$$

where $P_{sum}=\sum_{n=1}^{N}p_n$. (17) is equivalent to the following problem:

$$\begin{aligned}&\max_{p_n}\ f(P)-g(P)\\ &\text{s.t.}\quad C1: p_n \geq 0, \forall n\\ &\quad C2: \sum_{n=1}^{N} p_n \leq P_t,\\ &\quad C3: \sum_{n=1}^{N} p_n I_{n,l}^{SP} \leq I_l^{th}, \quad l=1,\ldots,L,\end{aligned} \tag{19}$$

where $f(P)=\log\eta_{SE}(P)$ and $g(P)=(1-\omega)\log(P_{sum}+P_c)$. The objective $f(P)-g(P)$ is a d.c. function as both $f(P)$ and $g(P)$ are concave. The gradient of $g(P)$ is $\nabla g(P)=\left(\frac{\partial g}{\partial p_1},\frac{\partial g}{\partial p_2},\ldots,\frac{\partial g}{\partial p_n}\right)$ where

$$\frac{\partial g}{\partial p_n}=\frac{1-\omega}{\sum_{n=1}^{N}p_n+P_c}. \tag{20}$$

Table 3 FW procedure.

FW procedure
1. **Initialization**
2. Set $t=0$, tolerance $\delta>0$
3. Find feasible point $P^{(0)}$, set $P^{(t)}=P^{(0)}$, calculate $V(P^{(0)})$
4. **Iteration**
5. Set $t=t+1$, $P^{(t)}=P^{(1)}$, calculate $V(P^{(1)})$.
6. **while** $\lvert V(P^{(t)})-V(P^{(t-1)})\rvert>\delta$
7. Solve (21) to obtain the optimal solution P^{*}.
8. Set $t=t+1$, $P^{(t)}=P^{*}$, calculate $V(P^{(t)})$.
9. **endwhile**

We propose an FW procedure [31-33] which generates a sequence of improved feasible solutions. Initialized from a feasible $P^{(0)}$, $P^{(t+1)}$ at tth iteration is generated as the optimal solution of the following convex optimization problem:

$$\max_{p_n} f(P)-g(P^{(t)})-<\nabla g(P^{(t)}),P-P^{(t)}>$$
$$\text{s.t.}\quad C1: p_n\geq 0,\forall n$$
$$C2: \sum_{n=1}^{N} p_n\leq P_t,$$
$$C3: \sum_{n=1}^{N} p_n I_{n,l}^{SP}\leq I_l^{th},\quad l=1,\ldots,L, \tag{21}$$

where $<x,y>=x^Ty$. The FW procedure to solve (19) is summarized in Table 3.

Function $g(P)$ is slowly sensitive to a change in the variable P, so $g(P)$ is well approximated by its first order approximation $g(P^{(t)})+<\nabla g(P^{(t)}),P-P^{(t)}>$ at a fairly large neighborhood of $P^{(t)}$. Thus the nonconvex optimization problem (19) is well approximated by the convex optimization problem (21).

As function $g(P)$ is concave, its gradient $g(P^{(t)})$ is also its super-gradient, so

$$g(P)\leq g(P^{(t)})+<\nabla g(P^{(t)}),P-P^{(t)}>. \tag{22}$$

Thus the convex optimization problem (21) provides a well approximated lower bound maximization for the nonconvex optimization problem (19). Besides, as

$$f(P^{(t+1)})-g(P^{(t+1)})\geq f(P^{(t)})-[g(P^{(t)}) + <\nabla g(P^{(t)}),P^{(t+1)}-P^{(t)}>]\geq f(P^{(t)})-g(P^{(t)}), \tag{23}$$

the next solution $P^{(t+1)}$ is always better than the previous solution $P^{(t)}$.

By Cauchy theorem, since the constraint set is compact, the sequence of improved solutions $\{P^{(t)}\}$ always converges. The iterative process terminates after finite iterations at $\lvert V(P^{(t)})-V(P^{(t-1)})\rvert\leq\delta$ with threshold ϵ.

4.4. Fast algorithm for optimizing (21)

Obviously, (21) defines a convex optimization problem. Generally, barrier method is a standard technique to solve convex optimization problems. For the barrier method, original problem is converted into a sequence of unconstrained minimization problems by defining a logarithmic barrier function with parameter t which decides the accuracy of the approximation. The solution to each minimization problem is called a central point in the central path related to the original problem. As t increases, the central point will be more and more close to the optimal solution of the original problem. For searching the center point with a given t, Newton method is generally employed. Therefor, the barrier method is always carried out via two essential steps, namely centering step and Newton step. The former is the outer iteration which is executed to compute the central point starting from the previously computed one. And the latter is the inner iteration implemented during each centering step [34].

To begin the barrier method, we reformulate the problem (21) into a set of unconstrained optimization problems by making all inequality constraints implicit in an objective function. The logarithmic barrier function is

$$\phi(x)=-\log\left(P_t-\sum_{n=1}^{N}p_n\right)-\sum_{l=1}^{L}\log\left(I_l^{th}-\sum_{n=1}^{N}p_n I_{n,l}^{SP}\right) -\sum_{n=1}^{N}\log(p_n), \tag{24}$$

where $x=(p_1,p_2,\ldots,p_N)$. Denote $Q(x)=f(P)-\sum_{n=1}^{N}\nabla g(P^{(t)})(p_n-p_n^{(t)})-g(P^{(t)})$. Thus, the optimal solution to (21) can be approximated by solving the following unconstrained minimization problem with a certain parameter t:

$$\min \psi_t(x)=-tQ(x)+\phi(x). \tag{25}$$

Eq. (25) can be solved efficiently by Newton method. The Newton step at x, denoted by Δx_{nt} is given by the following Karush-Kuhn-Tucker (KKT) systems:

$$\nabla^2\psi_t(x)\Delta x_{nt}=-\nabla\psi_t(x), \tag{26}$$

where $\nabla^2\psi_t(x)$ and $\nabla\psi_t(x)$ are the Hessian and the gradient of $\psi_t(x)$, respectively.

The computational complexity of the barrier method mainly lies in the computation of Newton step that needs matrix inversion. In order to reduce the computational cost, we exploit the structure of (25) and develop a fast algorithm to calculate the Newton step with lower complexity. Denote

$$f_0=P_t-\sum_{n=1}^{N}p_n$$
$$g_l=I_l^{th}-\sum_{n=1}^{N}p_n I_{n,l}^{SP},\quad l=1,2,\ldots,L. \tag{27}$$

The gradient of $\psi_t(x)$ is given by

$$\nabla\psi_t(x)=-t\left(\frac{H_n}{(1+p_nH_n)\sum_{n=1}^{N}\log(1+p_nH_n)}-\nabla g(p_n^{(t)})\right) +\frac{1}{f_0}+\sum_{l=1}^{L}\frac{I_{n,l}^{SP}}{g_l}-\frac{1}{p_n}, \tag{28}$$

where H_n is the SNR of the nth subchannel. The Hessian of $\psi_t(x)$ is

$$\nabla^2\psi_t(x) = \begin{bmatrix} D1 & & & \\ & D2 & & \\ & & \ddots & \\ & & & D_N \end{bmatrix} + \frac{\nabla f_0 \nabla f_0^T}{f_0^2} + \sum_{l=1}^{L} \frac{\nabla g_l \nabla g_l^T}{g_l^2}$$
$$= D + \sum_{i=1}^{M} F_i F_i^T. \quad (29)$$

where $M = L+1$ and $D = diag(D_1, D_2, \ldots, D_N) \in \mathcal{R}^{N\times N}$ with

$$D_n = \frac{tH_n^2(1+\sum_{n=1}^{N}\log(1+p_nH_n))}{(\sum_{n=1}^{N}\log(1+p_nH_n))^2(1+p_nH_n)^2} + \frac{1}{p_n^2}. \quad (30)$$

$F_i^{'}s$ are all vectors with N elements

$$F_i = \begin{cases} \frac{\nabla f_0}{f_0}, & i=1 \\ \frac{\nabla g_l}{g_l}, & l=1,\ldots,L, \quad i=l+1. \end{cases} \quad (31)$$

Since it is easy to prove that the matrix D is positive definite, it follows that the Hessian matrix $\nabla^2\psi_t(x)$ is invertible. However, if we compute the inversion of the KKT matrix directly, it has a complexity of $O(N^3)$, which is too high for application because there are thousands of OFDM subchannels in practical wireless systems.

Rewrite the KKT system (26) as follows:

$$\Lambda_0 \Delta x_{nt} = F_0, \quad (32)$$

where $\Lambda_0 = \nabla^2\psi_t(x)$ and $F_0 = -\nabla\psi_t(x)$. According to (29), Λ_0 can be written as

$$\Lambda_0 = D + \sum_{i=1}^{M} F_i F_i^T, \quad (33)$$

which can be decomposed into M equations

$$\Lambda_i = \Lambda_{i+1} + F_{i+1}F_{i+1}^T, \quad i = 0,1,\ldots,M-1, \quad (34)$$

By exploiting the structure of Λ_i's, we give an M-step procedure to compute the Newton step:

- *Step* 1: Use (34) to decompose Λ_0, $\Lambda_0 = \Lambda_1 + F_1F_1^T$. Denote two intermediate variables as the solutions of the following two sets of linear equations, $\Lambda_1 v_1^1 = F_0$ and $\Lambda_1 v_2^1 = F_1$. Then Δx_{nt} can be obtained by $\Delta x_{nt} = v_1^1 - \frac{F_1 v_1^1}{1+F_1 v_2^1} v_2^1$. So we can figure out μ if obtaining the two new variables v_1^1 and v_2^1.
- *Step* 2: Decompose Λ_1 with $\Lambda_1 = \Lambda_2 + F_2F_2^T$. Then the two variables introduced in step 1 can be updated by $v_i^1 = v_i^2 - \frac{F_2 v_i^2}{1+F_2 v_3^2} v_3^2, i = 1,2,$ where $\Lambda_2 v_i^2 = F_{i-1}$, $i = 1,2,3$.
- *Step m*: Decompose Λ_{m-1} with $\Lambda_m = \Lambda_m + F_m F_m^T$. We can update the m variables introduced in Step $m-1$ by $v_i^{m-1} = v_i^m - \frac{F_m v_i^m}{1+F_m v_{m+1}^m} v_{m+1}^m$, $i = 1,2,\ldots,m$, which is obtained by solving the following $m+1$ sets of linear equations, $\Lambda_m v_i^m = F_{i-1}$, $i = 1,2,\ldots,m+1$.

Continue the procedure to the Mth step, and there are $M+1$ matrix systems $\Lambda_M v_i^M = F_{i-1}$, $i = 1,2,\ldots,M+1$. From the derivation process, we can find that the m variables v_i^{m-1}, $i = 1,2,\ldots,m$ in the $(m-1)$th Step can be obtained by the $m+1$ variables v_i^m, $i = 1,2,\ldots,m+1$ in the mth Step. Thus, if we figure out the $M+1$ variables v_i^M, $i = 1,2,\ldots,M+1$, μ will be indirectly obtained.

Now we consider the matrix systems in step M. As $\Lambda_M = D$, these equations can be unified into

$$\begin{bmatrix} D1 & & & \\ & D2 & & \\ & & \ddots & \\ & & & D_N \end{bmatrix} v = h. \quad (35)$$

where $v, h \in \mathcal{R}^{N\times 1}$. Since D is a diagonal matrix, we can easily obtained

$$v_i = D_i^{-1} h_i, \quad i = 1,2,\ldots,N. \quad (36)$$

The computational complexity of obtaining v is $O(N)$. Thus it costs $O(NM)$ to solve the M variables at the Mth Step. Obviously, a reverse derivation of the M steps is necessary to figure out Δx_{nt} and the total computational complexity can be measured by $O(NM^2)$.

In practical CR systems, $M \ll N$ generally holds, so the complexity of the proposed algorithm is much lower than that of matrix inversion.

5. Simulation results

Experiments are conducted to evaluate the performance of our proposed scheme. Consider a multiuser OFDM-based CR system, where all users are randomly located in an area of 3×3 km, and the SU's receiver is distributed in a circle within 0.5 km from its transmitter. The path loss exponent is 4, the variance of the shadowing effect is 10 dB, and the multipath fading is assumed to be Rayleigh. The noise power on a subchannel is set to 10^{-13} W. The frequency bands occupied by PUs are generated randomly with the maximum number of OFDM subchannels $2W/3L$.

First, we investigate the convergence of our proposed algorithms. As discussed in Section 2.1, the computational load mainly lies in the computation of Newton step. Fig. 1 gives the Cumulative Distribution Function (CDF) of the number of Newton iterations for solving (21) in Section 2.1 with different settings of N. As seen in Fig. 2, the number of Newton iterations is small and varies in a narrow range, indicating our proposed algorithm is effective and efficient.

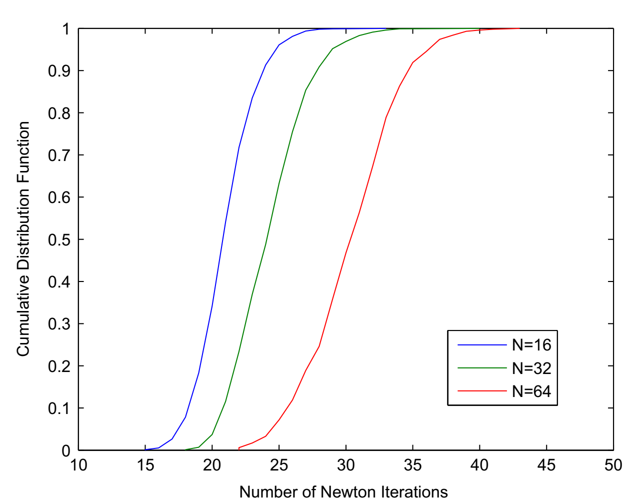

Fig. 1 CDF of the number of Newton iterations.

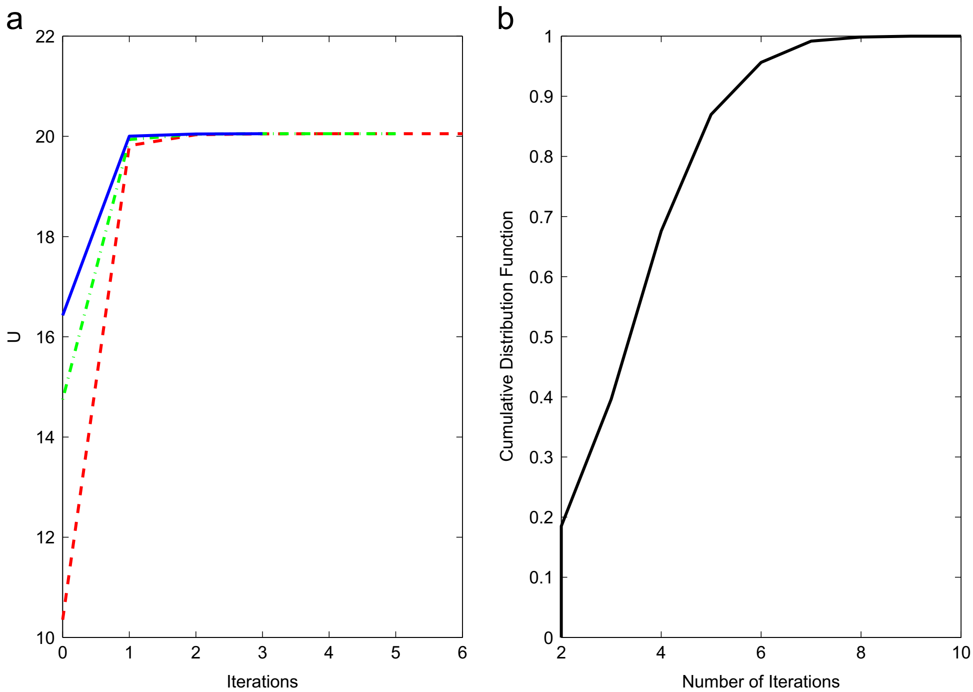

Fig. 2 Convergence of the utility function (with $N = 32$).

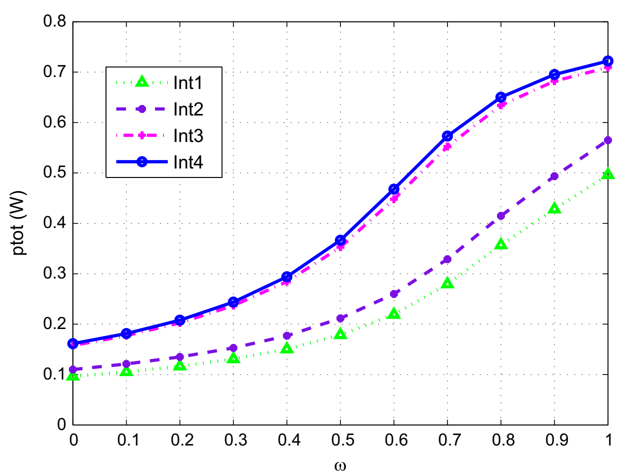

Fig. 3 The total transmit power (with $N = 32$ and $P_t = 0.8$ w).

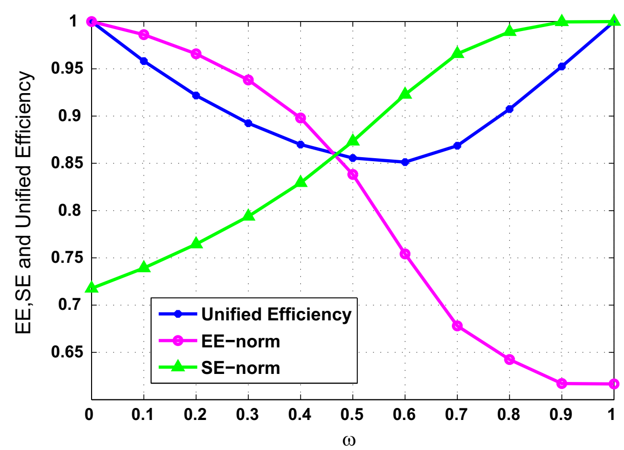

Fig. 4 SE-norm, EE-norm and U-norm under the optimal transmit power (with $N = 32$).

Fig. 2 illustrates the performance of the proposed FW procedure. The interference power threshold I_l^{th} are set to 5×10^{-12} W and $\omega = 0.5$. Fig. 2(a) shows that the FW procedure converges to the global optimal solution from different initial points. Fig. 2(b) gives the Cumulative Distribution Function (CDF) of the number of iterations for FW procedure to converge. As seen in Fig. 2, the number of iterations is small and varies in a narrow range, which shows the effectiveness and efficiency of the proposed algorithm.

Fig. 3 shows the total transmit power with the proposed EE-SE trade off metric. ω is set to 0.5. Int1, Int2, Int3 and Int4 represent the interference power threshold I_l^{th} are set to 2×10^{-12} W, 4×10^{-12} W, 6×10^{-12} W and 8×10^{-12} W, respectively. It is obviously that the transmit power is restricted by the power budget limitation and the interference constraints especially when ω is closed to 1.

Fig. 4 shows the normalized SE, EE and utility achieved with the optimal transmit power. The normalized SE, EE and utility are defined as

$$\eta_{SE}^{norm} = \frac{\eta_{SE}}{\eta_{SE}^{max}} \tag{37}$$

$$\eta_{EE}^{norm} = \frac{\eta_{EE}}{\eta_{EE}^{max}} \tag{38}$$

$$U^{norm} = [\eta_{SE}^{norm}]^{\omega} \times [\eta_{EE}^{norm}]^{1-\omega}. \tag{39}$$

It can be observed that the normalized SE (SE-norm) will be non-decreasing while the normalized EE (EE-norm) will be

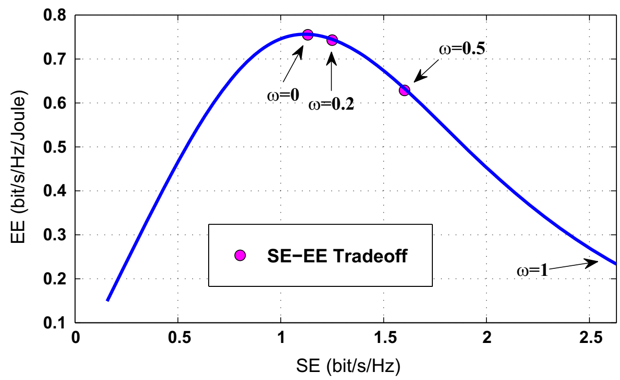

Fig. 5 EE-SE relationship (with $N=32$).

non-increasing with ω, and the intersection of the three lines is shown in Fig. 5. Furthermore, the normalized SE and EE will stay to be constants when ω is close to 1, which is because of the power constraints and interference constraints.

Fig. 5 illustrates the EE-SE relationship. It can be observed that maximal EE is achieved with $\omega=0$ while maximal SE is achieved with $\omega=1$. We can make a tradeoff between EE and SE for different preferences based on the EE-SE trade off metric. In other words, we can choose a certain ω for a practical system and then calculate the unique globally optimal solution according to the metric proposed in Section 3.

6. Conclusion

In this paper, we investigated the joint optimization problem of EE and SE in OFDM-based CR networks with imperfect spectrum sensing, which extended our preliminary research [35]. We formulated a multi-objective resource allocation problem to optimize the EE and the SE of a CR system simultaneously. We demonstrated the quasiconcavity of EE in SE, which characterizes the Pareto optimal set of the multi-objective optimization problem. A unified EE-SE tradeoff metric is introduced, based on which we can find a unique globally optimal solution. A fast algorithm is proposed to speed up the time-consuming computation by exploiting the structure of the problem. Simulation results validate the effectiveness of the proposed algorithms to obtain the unique globally optimal solution of the multi-objective optimization problem.

Acknowledgments

This work was partially supported by JiangsuSF (BK20151389) and the Fundamental Research Funds for the Central Universities (021014380013).

Appendix A. Proof of Theorem 1

Proof. Denote $\mathbf{R}_1^*$, $\mathbf{R}_2^*$ and $\mathbf{R}_3^*$ as the optimal rate vectors corresponding to the overall throughput R_1, R_2 and R_3, respectively, and they satisfy all constraints in (13). Without loss of generality, assume that $R_1<R_2<R_3$. Denote $\mathbf{R}_2$ as follows:

$$\begin{aligned}\mathbf{R}_2 &= \frac{R_3-R_2}{R_3-R_1}\mathbf{R}_1^* + \frac{R_2-R_1}{R_3-R_1}\mathbf{R}_3^* \\ &= \gamma\mathbf{R}_1^* + \gamma\mathbf{R}_3^*,\end{aligned} \tag{A.1}$$

where $\gamma=\frac{R_3-R_2}{R_3-R_1}$ and $0<\gamma<1$. It is obvious that $\mathbf{R}_2$ is in the feasible region of (13) and its sum rate is R_2. According to [36-38], $P^*(\mathbf{R})$ and $I(\mathbf{R})$ is strictly convex in $\mathbf{R}$, where $P^*(\mathbf{R})$ is the optimal power corresponding to the optimal rate vector $\mathbf{R}$ and $I(\mathbf{R})=\sum_{n=1}^{N}\frac{e^{r_n}-1}{H_n}I_{n,l}^{SP}-I_l^{th}$. Thus, $P^*(\mathbf{R}_2)<\gamma P^*(\mathbf{R}_1^*)+(1-\gamma)P^*(\mathbf{R}_3^*)$. Since $\mathbf{R}_2^*$ is the optimal rate vector corresponding to the overall throughput R_2, we have $P^*(\mathbf{R}_2^*)\le P^*(\mathbf{R}_2)$. So, we have $P^*(\mathbf{R}_2^*)<\gamma P^*(\mathbf{R}_1^*)+(1-\gamma)P^*(\mathbf{R}_3^*)$. Thus, for any given $R(=B\eta_{SE})$, the minimum transmit power $P^*(R)=P^*(\mathbf{R}^*)$ is strictly convex in R (and η_{SE}). Denote the super-level set of $\eta_{EE}^m(\eta_{SE})$ as $\mathbf{S}_\beta=\{R|\eta_{EE}^m(\eta_{SE})\ge\beta,\beta\le\mathcal{R}\}$. $\mathbf{S}_\beta$ is equivalent to $\{R|\beta P^*(\eta_{SE})+\beta P_c-\eta_{SE}\le 0\}$. As a result of the convexity of $P^*(\eta_{SE})$ proved above, $\mathbf{S}_\beta$ is strictly convex in η_{SE}. Thus, $\eta_{EE}^m(\eta_{SE})$ is strictly quasiconcave and has a unique global maximum. It is obvious that

$$\begin{aligned}\lim_{\eta_{SE}\to\infty}\eta_{EE}^m(\eta_{SE}) &= \lim_{\eta_{SE}\to\infty}\max_{\eta_{SE}}\frac{\eta_{SE}}{P^*(\eta_{SE})+P_c} \\ &= \lim_{P^*(\eta_{SE})\to\infty}\frac{o(P^*(\eta_{SE}))}{P^*(\eta_{SE})} \\ &= 0.\end{aligned} \tag{A.2}$$

Thus starting from $\eta_{SE}=0$, $\eta_{EE}^m(\eta_{SE})$ either strictly increases with η_{SE} if $\frac{d\eta_{EE}^m(\eta_{SE})}{d\eta_{SE}}|_{\eta_{SE}=\eta_{SE}^{max}}\ge 0$ or first strictly increases and then strictly decreases with η_{SE} if $\frac{d\eta_{EE}^m(\eta_{SE})}{d\eta_{SE}}|_{\eta_{SE}=\eta_{SE}^{max}}<0$. The maximum EE in the SE region $[0,\eta_{SE}^{max}]$ is straightforward as indicated in Theorem 1.□

Appendix B. Proof of Theorem 2

Proof. If $\eta_{SE}^*\ge\eta_{SE}^{max}$, $\eta_{EE}^m(\eta_{SE})$ is increasing at $[0,\eta_{SE}^{max}]$ according to Theorem 1. Thus $\forall\eta_{SE}\in[0,\eta_{SE}^{max})$, we have $\eta_{EE}^m(\eta_{SE}^{max})>\eta_{EE}^m(\eta_{SE})$ and $\eta_{SE}^{max}>\eta_{SE}$, which results in $P^{POS}=\{P|\eta_{SE}=\eta_{SE}^{max}\}$. If $\eta_{SE}^*<\eta_{SE}^{max}$, $\eta_{EE}^m(\eta_{SE})$ is increasing at $[0,\eta_{SE}^*)$ while decreasing at $[\eta_{SE}^*,\eta_{SE}^{max}]$ due to Theorem 1. $\forall\eta_{SE}\in[0,\eta_{SE}^*)$, we have $\eta_{EE}^m(\eta_{SE}^*)>\eta_{EE}^m(\eta_{SE})$ and $\eta_{SE}^*>\eta_{SE}$, which means $\{P|0\le\eta_{SE}<\eta_{SE}^*\}\cap P^{POS}=\varnothing$. However, $\forall P\in\{P|\eta_{SE}\in[\eta_{SE}^*,\eta_{SE}^{max}]\}$, there does not exist any other point P' such that $\eta_{EE}^m(\eta_{SE}(P'))>\eta_{EE}^m(\eta_{SE}(P))$ and $\eta_{SE}(P')>\eta_{SE}(P)$. Thus, $P^{POS}=\{P|\eta_{SE}^*\le\eta_{SE}\le\eta_{SE}^{max}\}$.

References

[1] FCC, Facilitating Opportunities for Flexible, Efficient, and Reliable Spectrum Use Employing Cognitive Radio Technologies, FCC Report ET Docket 03-322.

[2] S. Haykin, Cognitive radio: brain-empowered wireless communications, IEEE J. Sel. Areas Commun. 23 (2) (2005) 201-220.

[3] L. Liu, Y. Zhou, L. Tian, J. Shi, Cpc-based backward-compatible network access for lte cognitive radio cellular networks, IEEE Commun. Mag. 53 (7) (2015) 93-99. http://dx.doi.org/10.1109/MCOM.2015.7158271.

[4] Y. Zhou, H. Liu, Z. Pan, L. Tian, J. Shi, Spectral- and energy-efficient two-stage cooperative multicast for lte-advanced and

beyond, IEEE Wireless Commun. 21 (2) (2014) 34–41. http://dx.doi.org/10.1109/MWC.2014.6812289.

[5] T.A. Weiss, F.K. Jondral, Spectrum pooling: an innovative strategy for the enhancement of spectrum efficiency, IEEE Commun. Mag. 42 (3) (2004) 8–14.

[6] R. Zhang, Y.-C. Liang, S. Cui, Dynamic resource allocation in cognitive radio networks, IEEE Signal Process. Mag. 27 (3) (2010) 102–114.

[7] C. Sacchi, F. Granelli, C. Schlegel, A qoe-oriented strategy for ofdma radio resource allocation based on min-mos maximization, IEEE Commun. Lett. 15 (5) (2011) 494–496.

[8] S. Wang, Efficient resource allocation algorithm for cognitive OFDM systems, IEEE Commun. Lett. 14 (8) (2010) 725–727.

[9] M. Ge, S. Wang, Fast optimal resource allocation is possible for multiuser OFDM-based cognitive radio networks with heterogeneous services, IEEE Trans. Wireless Commun. 11 (4) (2012) 1500–1509.

[10] S. Wang, Z.-H. Zhou, M. Ge, C. Wang, Resource allocation for heterogeneous multiuser OFDM-based cognitive radio networks with imperfect spectrum sensing, in: Proceedings of the IEEE INFOCOM'12, Orlando, FL, 2012, pp. 2264–2272.

[11] C. Han, T. Harrold, S. Armour, I. Krikidis, S. Videv, P. Grant, H. Haas, J. Thompson, I. Ku, C.-X. Wang, T.A. Le, M. Nakhai, J. Zhang, L. Hanzo, Green radio: radio techniques to enable energy-efficient wireless networks, IEEE Commun. Mag. 49 (6) (2011) 46–54.

[12] Y. Chen, S. Zhang, S. Xu, G. Li, Fundamental trade-offs on green wireless networks, IEEE Commun. Mag. 49 (6) (2011) 30–37.

[13] S. Althunibat, R. Palacios, F. Granelli, Energy-efficient spectrum sensing in cognitive radio networks by coordinated reduction of the sensing users, in: Proceedings of the IEEE ICC'12, Ottawa, Canada, 2012, pp. 1399–1404.

[14] E. Oh, B. Krishnamachari, X. Liu, Z. Niu, Toward dynamic energy-efficient operation of cellular network infrastructure, IEEE Commun. Mag. 49 (6) (2011) 56–61.

[15] A. Zappone, G. Alfano, S. Buzzi, M. Meo, Energy-efficient noncooperative resource allocation in multi-cell OFDMA systems with multiple base station antennas, in: Proceedings of the IEEE GreenCom'11, 2011, pp. 82–87.

[16] C. Coskun, E. Ayanoglu, Energy-efficient base station deployment in heterogeneous networks, IEEE Wireless Commun. Lett. 3 (6) (2014) 593–596.

[17] W. Feng, H. Alshaer, J. Elmirghani, Green information and communication technology: energy efficiency in a motorway model, IET Commun. 4 (7) (2010) 850–860.

[18] Y. Chen, S. Zhang, S. Xu, G. Li, Fundamental trade-offs on green wireless networks, IEEE Commun. Mag. 49 (6) (2011) 30–37.

[19] Y. Wu, Y. Chen, J. Tang, D. So, Z. Xu, I. Chih-Lin, P. Ferrand, J.-M. Gorce, C.-H. Tang, P.-R. Li, K.-T. Feng, L.-C. Wang, K. Borner, L. Thiele, Green transmission technologies for balancing the energy efficiency and spectrum efficiency trade-off, IEEE Commun. Mag. 52 (11) (2014) 112–120.

[20] C. Xiong, G. Li, S. Zhang, Y. Chen, S. Xu, Energy- and spectral-efficiency tradeoff in downlink OFDMA networks, IEEE Trans. Wireless Commun. 10 (11) (2011) 3874–3886.

[21] C. He, B. Sheng, P. Zhu, X. You, G. Li, Energy- and spectral-efficiency tradeoff for distributed antenna systems with proportional fairness, IEEE J. Sel. Areas Commun. 31 (5) (2013) 894–902.

[22] L. Deng, Y. Rui, P. Cheng, J. Zhang, Q. Zhang, M. Li, A unified energy efficiency and spectral efficiency tradeoff metric in wireless networks, IEEE Commun. Lett. 17 (1) (2013) 55–58.

[23] G. Bansal, M. Hossain, V. Bhargava, Adaptive power loading for OFDM-based cognitive radio systems, in: Proceedings of the IEEE ICC'07, Glasgow, Scotland, 2007 pp. 5137–5142.

[24] X. Zhou, G. Li, D. Li, D. Wang, A. Soong, Probabilistic resource allocation for opportunistic spectrum access, IEEE Trans. Wire. Commun. 9 (9) (2010) 2870–2879.

[25] H. Zhang, Z. Zhang, H. Dai, R. Yin, X. Chen, Distributed spectrum-aware clustering in cognitive radio sensor networks, in: Proceedings of the IEEE GLOBECOM'11, Houston, TX, 2011 pp. 1–6.

[26] D. Chen, S. Yin, Q. Zhang, M. Liu, S. Li, Mining spectrum usage data: a large-scale spectrum measurement study, in: Proceedings of the ACM MOBICOM'09, Beijing, China, 2009, pp. 13–24, http://dx.doi.org/10.1145/1614320.1614323.

[27] L. Lu, X. Zhou, U. Onunkwo, G. Li, Ten years of research in spectrum sensing and sharing in cognitive radio, EURASIP J. Wire. Commun. Netw. 2012 (28) (2012) 1–16.

[28] A.J. Goldsmith, S. Chua, Variable-rate variable-power MQAM for fading channels, IEEE Trans. Commun. 45 (10) (1997) 1218–1230.

[29] S. Cui, A. Goldsmith, A. Bahai, Energy-constrained modulation optimization, IEEE Trans. Wireless Commun. 4 (5) (2005) 2349–2360.

[30] S. Wang, F. Huang, Z. Zhou, Fast power allocation algorithm for cognitive radio networks, IEEE Commun. Lett. 15 (8) (2011) 845–847.

[31] M. Frank, P. Wolfe, An algorithm for quadratic programming, Naval Res. Log. Quart. 3 (1–2) (1956) 95–110.

[32] P. Apkarian, H.D. Tuan, Robust control via concave minimization local and global algorithms, IEEE Trans. Autom. Control 45 (2) (2000) 299–305.

[33] H. Kha, H. Tuan, H. Nguyen, Fast global optimal power allocation in wireless networks by local d.c. programming, IEEE Trans. Wireless Commun. 11 (2) (2012) 510–515.

[34] S. Boyd, L. Vandenberghe, Convex Optimization, Cambridge University Press, New York, 2004.

[35] W. Shi, S. Wang, D. Chen, Energy- and spectrum-efficiency tradeoff in ofdm-based cognitive radio systems, in: Proceedings of the IEEE GLOBECOM'14, Austin, TX, 2014, pp. 3092–3097, http://dx.doi.org/10.1109/GLOCOM.2014.7037280.

[36] W. Yu, R. Lui, Dual methods for nonconvex spectrum optimization of multicarrier systems, IEEE Trans. Commun. 54 (7) (2006) 1310–1322.

[37] Z.-Q. Luo, S. Zhang, Dynamic spectrum management: complexity and duality, IEEE J. Sel. Top. Signal Process. 2 (1) (2008) 57–73.

[38] K. Seong, M. Mohseni, J. Cioffi, Optimal resource allocation for OFDMA downlink systems, in: Proceedings of the IEEE ISIT'06, Seattle, WA, 2006, pp. 1394–1398.